Electron trapping induced proton uptake: a general factor leading to photoactivity decay of nanostructured TiO_2

Tao He,*[1] Libo Wang,[1] Francisco Fabregat-Santiago,*[2] Ying Li,[1] Chong Wang,[3] Guoqun Liu[4]

* *co-corresponding authors*

[1] *College of Chemistry and Chemical Engineering,* [3]*College of Optoelectronic Information Science and Technology, Yantai University, China.*

[2] *Photovoltaic and Optoelectronic Devices Group, Institute of Advanced Materials, Universitat Jaume I, 12006 Castelló, Spain.*

[4] *School of Materials and Chemical Engineering, Zhongyuan University of Technology, China*.

Abstract In most photoactive semiconductors photochemical corrosion, which leads to photoactivity decay, is one of the bottleneck problems for their realistic application. Herein, we will disclose that electron trapping induced proton uptake is a general factor leading to photoactivity decay of nanostructured TiO_2 which is known for its exceptionally high photochemical stability. By using both phenolphthalein and phosphate group with covalent P-O-Ti connections as molecular probes and application of combined electrochemical techniques, the occurrence of electron trapping induced proton uptake and the mechanism of the photoactivity decay are investigated. This research reveals an important but easily overlooked fact, that is, the carriers' kinetics in nanostructured TiO_2 may not be able to reach a steady state. In other words, a stable photocurrent may not be obtained because the photoelectrochemical process will alter the carriers' dynamics continuously, which leads to continuous decay of the photocurrent. This result could be also common with other semiconductors.

1. Introduction

Nanostructured TiO_2 is an important photoactive semiconductor and widely used in various photoelectrochemical (PEC) processes including photovoltaic cells[1], organic pollution degradation[2-5], water splitting[6-8] and biosensors[9-10]. These promising application potentials rest not only on its excellent photoelectric properties and the exceptionally large specific surface area, but also on the high photochemical stability which is usually the first requirement for realistic applications. In fact, TiO_2 is among the known photoactive semiconductors showing the highest stability against photochemical corrosion.

However, even for TiO_2, it is still common to find a continuous decay of the photoactivity in various PEC processes.[11-14] For example, continuous photocurrent attenuation during the chronoamperometric (i-t) test usually occurs. To our knowledge, so far no research has declared that a constant photocurrent value can be reached after a long duration of static photo irradiation. This kind of photoactivity decay is generally assigned to continuous increase of recombination associated to the

increasing accumulation of photo-generated carriers trapped in intra band gap states and oxidizing active species formed at semiconductor/electrolyte interface.[11-14] However, a more in-depth understanding about the mechanism of the photoactivity decay is still lacking. Considering its generality, it is necessary to answer this question before countermeasures can be developed.

It is known that surface defect states can exert heavy influence on both the thermodynamics and kinetics of PEC processes.[15-19] They may cause Fermi level pinning or partial pinning in some nanostructured photoelectrodes,[15] which is responsible of increasing the overpotential needed for PEC water oxidation.[16-17] On the other hand, during PEC processes these sites may act as recombination sites[18] or active sites for hole interface transfer (water oxidation) reactions.[19] In this work, we will demonstrate for the first time that surface defect states may exert another important influence on the dynamics of electrons in TiO_2 electrode which leads to the general photoactivity decay.

In order to reveal the general decay mechanism, two typical nanostructured TiO_2 photoelectrodes are prepared, one is single crystal nanorod array with less defect states and the other is nanoparticulate film with much higher amount of defect states. By using both phenolphthalein and phosphate group with covalent P-O-Ti connections as molecular probes, we substantiate that electron trapping in intrabandgap states can lead to electrostatic adsorption of protons from electrolyte solution. Insertion of protons or other small cations such lithium under negative bias is known to produce structural changes in TiO_2 leading to conduction band edge movements, increases in conductivity and changes in color.[20-22] Based on comparative studies on their structures and PEC properties of the two TiO_2 photoelectrodes, we propose that the electrostatic attraction between the trapped electrons and adsorbed cations lead to continuous increase of electron transport resistance and recombination, which consequently results in the general photoactivity decay.

2. Experimental section

2.1 Preparation and characterization of two types of nanostructured TiO_2 films

Single crystalline *rutile* TiO_2 nanorod arrays are grown hydrothermally on the conducting surface of FTO substrates (the film is called R-TiO_2)[23]. The nanoparticulate films on FTO substrates are prepared through the common "doctor blade" processing and sintering procedure, the raw materials are *anatase* TiO_2 nanoparticles prepared through a dialysis procedure[24] (the film is called D-TiO_2). X-ray diffraction (XRD, Shimadzu-6100 diffractometer with a Cu Kα radiation) and scanning electron microscopy (SEM, HITACHI S-4800 FE-SEM) techniques are applied to give structural and morphological characterizations of the films.

2.2 Electron trapping experiments

All the electrochemical and photoelectrochemical experiments are carried out by using a CHI electrochemical analyzer (CHI660E) with a standard three-electrode

system. 1 cm^2 TiO_2 films are the working electrodes; a probe of Ag/AgCl, KCl saturated (218; Shanghai Leici Inc.), placed 5 mm away from the surface of the TiO_2 film, is reference electrode; a 2 cm^2 Pt sheet serves as the counter electrode. 1.0M KNO_3 solution is used as the electrolyte. All of the potential values given herein are referenced to the Ag/AgCl electrode. "Electron trapping" experiments are carried out by applying a negative bias (-0.6~-0.9V) to the TiO_2 films and keeping at this potential for a certain period of time. The KNO_3 solution in the PEC cell is bubbled for 30 minutes to eliminate O_2 before experiments. In order to verify "electron trapping" induced electrostatic adsorption of protons, two separate "electron trapping" experiments are carried out, respectively. One is that 3 drops of solution of phenolphthalein dissolved in ethanol (0.5wt%) are added into the KNO_3 electrolyte before the experiment and then the color changing of the TiO_2 electrode is recoded during the "electron trapping" experiment. The other is that phosphate-modified TiO_2 nanoparticulate electrodes[25] are used to carry out the "electron trapping" experiment". The TiO_2 powders scraped out of the phosphate-modified TiO_2 film before and after the "electron trapping" experiment and mixed with KBr to prepare the IR samples, IR spectra are measured with Fourier transform infrared spectroscopy (Shimadzu IRAffinity-1).

2.3 Photo/electrochemical measurements

Chronoamperometric measurements (i-t) under super band gap irradiation are carried out by using a LED lamp (LHFC084−10, 365 nm, 0.6 W/cm^2, Shenzhen Lamplic Science Co., Ltd.) connected to a controller (UVEC-4II, Shenzhen Lamplic Science Co., Ltd.) as the light source.

In order to explore the mechanism of the continuous photocurrent decay, we design a series of combined photoelectrochemical measurement schemes. The main idea is to track the time-dependent evolution of the photoactive-determining parameters along with the proceeding of PEC process. For example, impedance measurement in dark is carried out immediately after a certain period of i-t measurement under static UV irradiation, which allows us to investigate the alterations of the conduction band during the PEC process.

3. Results and discussion

3.1 General and continuous photoactivity decay of nanostructured TiO_2

Figure 1 shows the i-t curves of the D-TiO_2 and R-TiO_2 films under static UV irradiation. All ~~of~~ the curves feature a photocurrent spike appearing at the beginning of UV light irradiation and then a continuous and slow attenuation of the photocurrent even if the PEC process proceeds for more than 10 minutes. The initial photocurrent spikes which are very common during i-t measurements are resulted primarily from photogenerated electrons being trapped in intra band gap states (and other capacitive contribution such as Helmoholtz capacitance) and not because of real PEC reactions such as water splitting. The decay rate of the photocurrent is different when different TiO_2 photoelectrode is used (Figure 1a and b). Moreover, the UV light was checked

with a UV sensor (UV-A, Photoelectric Instrumental Factory of Beijing Normal University), precluding that the photocurrent decay is because of the attenuation of UV light intensity. Therefore, the continuous drops of the photocurrent after the spikes are indicative of photoactivity decay of the photoelectrodes. Compared to D-TiO_2, the R-TiO_2 film shows much higher photocurrent and much slower photocurrent decay. With the photocurrent at 100s as the initial value, the decays at 500s are respectively 7.7% for R-TiO_2 and 16.9% for D-TiO_2 film.

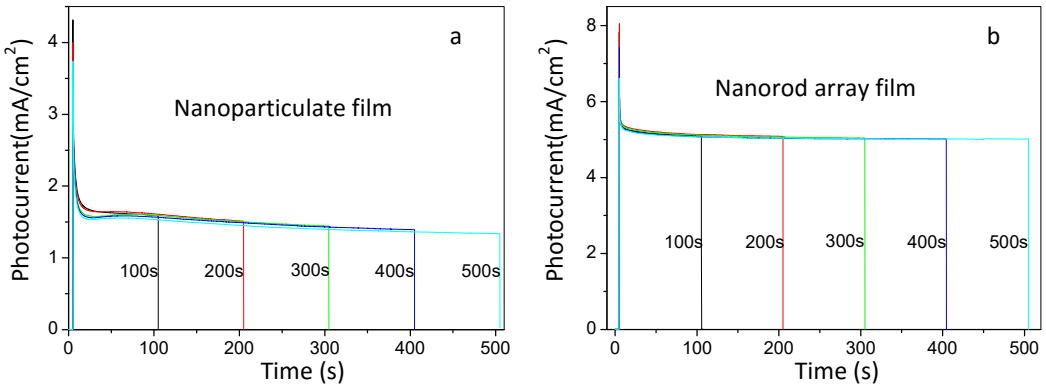

Figure 1. i-t curves of (a) D-TiO_2 and (b) R-TiO_2 electrodes measured under continous UV irradiation for five different period of times. The electrolyte is 1.0 M KNO_3, potential bias is +0.6 V vs Ag/AgCl.

A remarkable characteristic of the photocurrent decay lies in the reversibility, that is, the i-t curves from multiple parallel measurements can be nearly coincided (Figure 1a and b). The complete recovery of the initial photocurrent value from repeating measurements definitely excludes the possibility that the photoactivity decay is resulted from irreversible photocorrosion commonly encountered for many other non-TiO_2 semiconductor photoelectrodes. I-t measurements are also carried out with some other type of TiO_2 films, or in different electrolytes, or with the addition of hole scavengers, the i-t curves always feature a continuous photocurrent decay. Factually, this kind of photocurrent decays are very common and have also been reported by different research groups during the past 20 years.[11-14]

Since the continuous photocurrent decay is related to neither light source nor electrolyte, it is probably resulted from some continuous change at the semiconductor/electrolyte interface. Moreover, the change should be general and reversible. It is known that nanostructured semiconductors usually have great high density of surface defect states.[15-19] These defect states may cause Fermi level pinning.[15] Under this circumstance, the applied bias is mainly consumed at the electrolyte side to change the potential distribution in Helmholtz layer. As a result, the performance will be impaired due to the energy band bending and photovoltage become smaller.[17]

After the i-t processes under UV exposure proceed for different periods of time, cyclic voltammetry (CV) or Mott-Schottky (M-S) measurements in dark are carried out

immediately (Figures s1 and s2). The combined measurements are controlled automatically by computer with macro command programs, and there is no time interval between the two measurements (i-t/CV or i-t/M-S). All these measurements give strong evidences that the electrode/electrolyte interface can quickly reach a static quasi-equilibrium status during the PEC process and the energy band edges are fixed. The band edge pinning is common in metal oxide semiconductor/electrolyte systems where the density of the surface defect states is not too high and the electrolyte concentration is not too low. Since the energy band edges are fixed after initial shift (in other words, no Fermi level pinning occurs) (Figures s1 and s2) while photocurrent decay continues (Figure 1), there is no correlation between them. Therefore, we shift our attention to carriers' dynamic behaviors.

3.2 Occurrence of ETPU

Nanostructured TiO_2 usually have strong tendency to trap electrons due to high chemical capacitance of band gap states (C_μ).[20,26,27] It is reasonable to think that TiO_2 can be negatively charged if electrons are trapped in band gap states. Moreover, it has long been realized that electron trapping in band gap states can induce proton (or other cation ions) charge compensation uptake (call ETPU).[28] Herein, we propose and further verify for the first time that it is the ETPU process that leads to the general and continuous photocurrent decay.

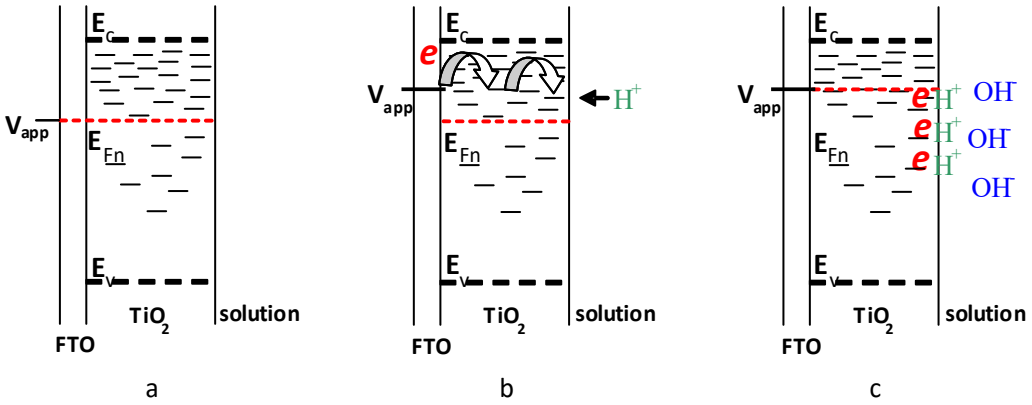

Figure 2. Schematic illustrations of (a) the FTO|TiO_2|electrolyte system，(b) electron trapping induced proton (H^+) uptake and (c) ETPU induced OH^- excess in solution side. The red dashed line marks the E_{Fn}, the trap states (short lines) above or below the E_{Fn} are unpopulated or populated.

PEC process involves complicated dynamic processes of charge carriers in both semiconductor and electrolyte and thus can not give direct evidence of ETPU. Herein, electron trapping in TiO_2 intra band gap states is realized by applying negative potentials to TiO_2 electrodes in dark condition. Under this simple electrochemical system, applied potential V_{app} (corresponding to electron Fermi level, E_{Fn}) is the only variable to be adjusted to control the population of trap states (Figure 2a and b). Thus, the influence of electron trapping on the system can be easily detected.

In neutral electrolytes (pH=7), ETPU will lead to OH^- excess in solution side (see

Figure 2c) which thus can be used as a criterion for the occurrence of ETPU. However, pH meter is failed to detect such a change, which indicates that if ETPU really happens the OH^- excess may only appear in a very thin layer of solution close to the interface. Thus, new method which can detect pH variation in this microdomain is needed.

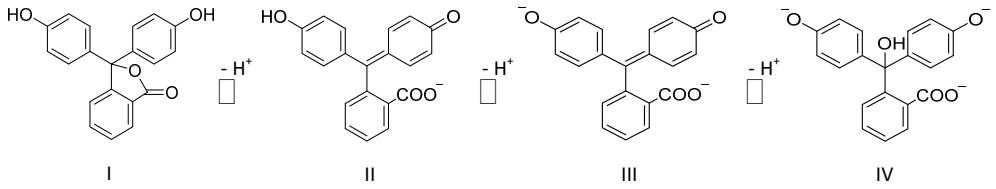

Figure 3. Schematic illustrations of phenolphthalein coloration process. In neutral or weak acid solution, it has a lactone structure (I) which is colorless. In weak base solution, it loses one or two protons yielding to quinine structures (II or III) which show red color. The quinine structure in strong base solution will further transform into the colorless methanol-type structure (IV).

Phenolphthalein ($C_{20}H_{14}O_4$) is one of the important and most commonly used acid-base indicator.[29] The color-changing mechanism is due to reversible transform of the molecular structures in different pH environments (Figure 3). Considering its high sensitivity to pH variation and appropriate color change interval (pH 8~10) we select it as the probe to test the ETPU-induced pH change at TiO_2/electrolyte interface.

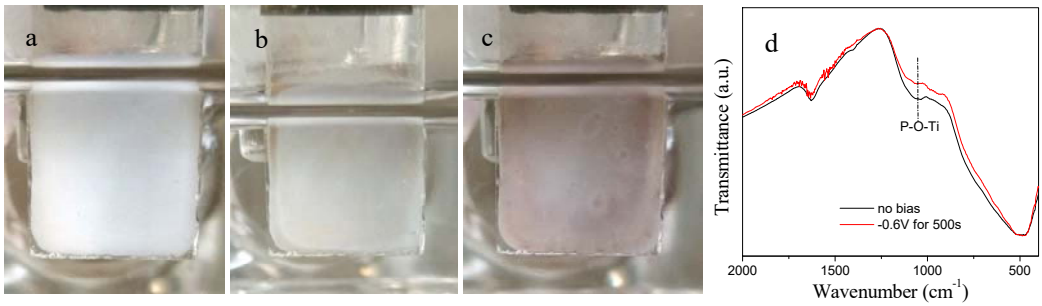

Figure 4. Pictures of the D-TiO_2 electrode in PEC cell, (a) before electron trapping experiment and with phenolphthalein in electrolyte; (b) during electron trapping and without phenolphthalein in electrolyte; (c) during electron trapping and with phenolphthalein in electrolyte. (d) IR spectra of the phosphate-modified TiO_2 before and after subjecting to the "electron trapping" experiment. Note that the "electron trapping" experiments are carried out under anaerobic condition.

The pictures in Figure 4 record the color change of the TiO_2 electrodes during the electron trapping process. If without phenolphthalein in electrolyte, the color of the film after applying a -0.9V bias will change from white to light gray due to the light absorption of electrons in conduction band and trap states of TiO_2 and also to the color change associated to proton insertion in TiO_2 (Figure 2a and b).[30,31] On the

contrary, the color of the film turns gradually from white to pink if phenolphthalein is added beforehand, indicating a weak base condition is formed (Figure 4c). Moreover, the pink color can only be detected in the surface of the TiO_2 film. Therefore, the OH^--excess condition at the interface of TiO_2/electrolyte definitely proves the occurrence of ETPU.

As for the color changing experiments, another three important issues should be pointed out. Firstly, the TiO_2 films have a highly nanoporous structure (see the following SEM images, Figure 6) which contribute to the vast majority of the TiO_2/electrolyte interface. It means that the ETPU-induced OH^- excess mainly occurs within the nanoporous framework which may hinder the diffusion of OH^- towards bulk solution and thus lead to the increase of pH within the confined domains. Also note that the color changing reaction of phenolphthalein is sensitive to pH alteration and it only needs 1 pH unit change (from 7 to 8) to make the colorless phenolphthalein solution turn into red. Secondly, a very high OH^--excess condition (strong base condition) which is necessary for phenolphthalein to transform to the colorless methanol-type structure (IV) cannot be satisfied by the ETPU-induced OH^- excess. It is because that the limited number of band gap states in the thin TiO_2 film cannot uptake too much protons. As a result, the pink color does not disappear even if a long period (500s) of electron trapping at -0.9V is applied (note that chronoamperometric test proves that -0.9V can not initiate water electrolysis reaction, that is, no OH^- ion is formed through the reaction $H_2O + e^- = OH^- + 1/2H_2$). Finally, the pink color disappears instantly as long as the applied bias is shift to a positive potential of +0.6V (please check the supporting information for the video file which recorded the instant color changing process). At this positive bias, the trapped electrons leave TiO_2 and flow back to external circuit, at the same time the adsorbed protons reenter the electrolyte solution. As a result, the neutral pH condition at the TiO_2/interface is regained and the indicator molecules restore the initial colorless lactone structure (I). This color-changing experiment proves that the ETPU is a reversible process and further confirms that the OH^- excess is not because of the irreversible water electrolysis reaction.

Applying a large negative bias to TiO_2 electrodes can initiate irreversible covalent bonding of protons with lattice oxygen, which can remarkably improve the conductivity of TiO_2 due to the great increase of donor densities.[32-34] While, the ETPU can not initiate irreversible O-H bonding, as the energy levels of these band gap states are too low. Therefore, the nature of ETPU should be of electrostatic interaction, which endows ETPU with its reversible character. The instant color changing give us another evidence that most protons are probably not inserted into TiO_2 lattice but adsorbed electrostatically on TiO_2 surface. Otherwise, it should take a certain amount of time for the protons to be released. Therefore, the adsorbed protons should be mainly located at surface defect and/or grain boundary defect sites where electrons are simultaneously trapped, which has been described by Boschloo as the origin of “shallow” energy localized states associated to Ti^{3+} in the lattice.[30,35]

It is well known that phosphate groups can be chemically adsorbed to TiO_2 surface through covalent Ti-O-P connections which show characteristic absorptions centered at ca. 1050 cm^{-1} in IR spectra (Figure 4d).[24,25,36] It has been proven that the hydrolysis of Ti-O-P connections can only occur in alkaline solution but cannot in neutral or acidic solution.[37] IR spectra indicate the dissociation of the covalent Ti-O-P connection after a phosphate-modified TiO_2 electrode is subjected to the electron trapping experiment, further confirming the occurrence of the ETPU process (see Figure s3 for more details).

3.3 ETPU induced photoactivity decay

It has been revealed that electron transport is usually 10^3~10^5 times slower in nanoparticulate film than in single crystal.[38,39] Two main reasons are usually considered.[39] Firstly, structural disorder at grain boundary causes enhanced scattering of free electrons with lattice, which reduces the electron mobility. Secondly, the surface trap states with large distribution in energy take part in electron transport through the "trapping-detrapping" events which is much slower than the transport of free electron in conduction band.

Apparently, for a given film the lattice scattering effect due to structural disorder will be kept unchanged, while the "trapping-detrapping" dynamics can be altered because the trap states may be modified during PEC process. It is reasonable to think the electrostatic attractions between trapped electrons and protons will increase the energy barrier of detrapping. Within the framework of the multiple trapping mode, the energy barrier for the trapped electrons to detrap to extended states determines the transport property of electrons in nanostructured semiconductors.[38-40]

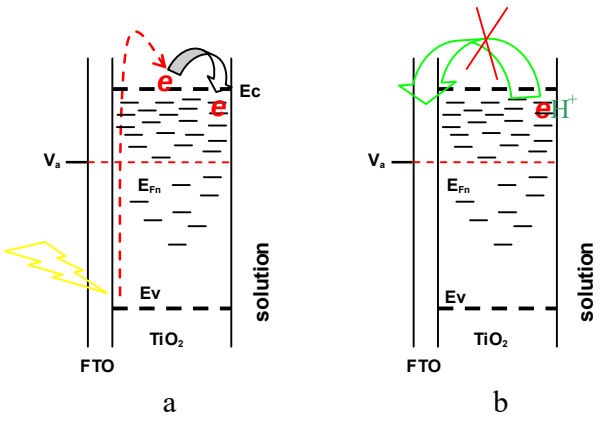

Figure 5. Schematic diagrams, (a) photogenerated electrons trapping in band gap states; (b) the electrostatic interaction between trapped electron and adsorbed proton making electron unable to be detrapped.

Based on the above consideration, we propose the following mechanism to explain the general and continuous photocurrent decays (Figure 5): Along with the proceeding of PEC process, ETPU occurs continuously. More and more trapped electrons have enlarged detrapping barriers due to the electrostatic interaction between trapped

electrons and adsorbed protons. Consequently, recombination will continuously increase because electron transport property continuously deteriorates and trapped electrons have prolonged residence time. In order to substantiate this mechanism, two critical aspects need to be verified. One is that a film with much higher density of surface defect states should have much faster photocurrent decay. The other is that a continuous increase of electron transport resistance must be detected.

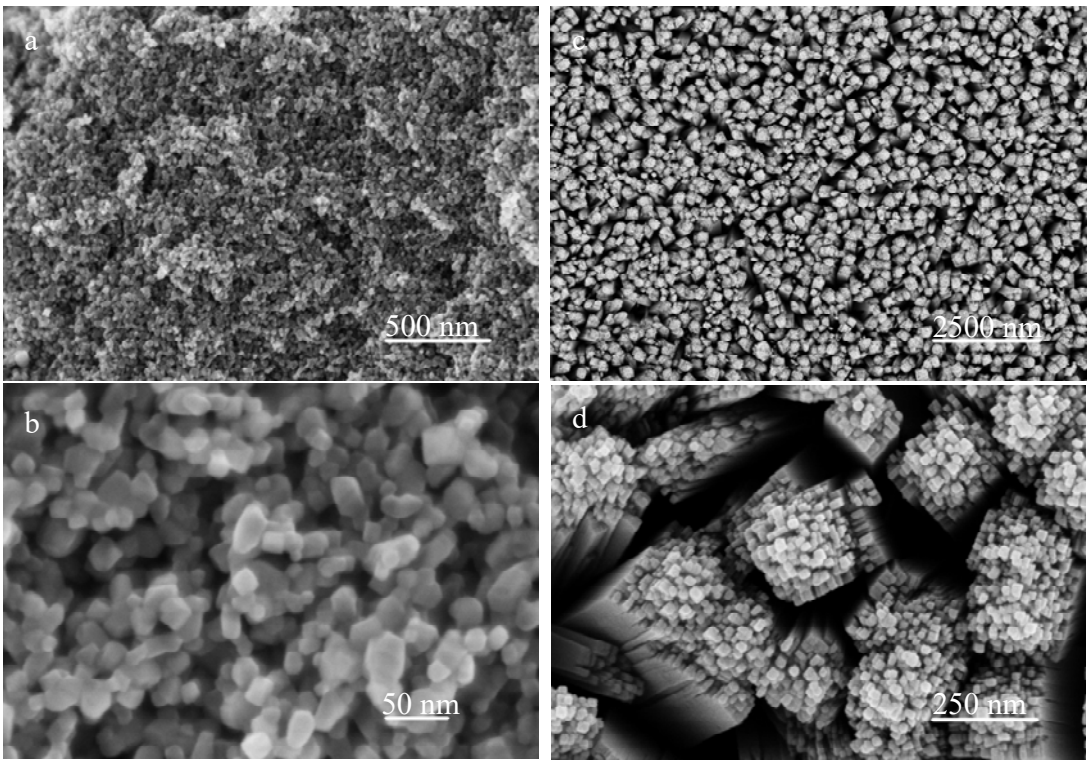

Figure 6. SEM images of D-TiO_2 (a) and (b) and R-TiO_2 (c) and (d) films.

The SEM images show the stark contrast in nanostructures of the two film electrodes, D-TiO_2 and R-TiO_2 (Figure 6). The former is constructed through a random aggregation of anatase TiO_2 nanocrystals with a size of 10~30 nm, which leads to the formation of nanopores highly dispersed within the film (Figure 6a, b). While, R-TiO_2 film is composed of an array of rutile TiO_2 single crystal rods with a diameter of 200nm and the axial [001] direction perpendicular to FTO surface (see Figure s4 for XRD spectra of the films).

The structural differences imply that D-TiO_2 film have much larger density of surface and grain boundary defect states. This conclusion is substantiated by the CV (Figure s1a and b) as well as the potential step chronoamperometry measurements (Figure s5e) which all indicate that D-TiO_2 has much larger chemical capacitance associated to traps (Note that the TiO_2 amount in D-TiO_2 film was adjusted to the same with that in R-TiO_2 film during preparation, *ca.*0.0030g/cm^2). Therefore, the first critical inference to support our proposed mechanism about the continuous photoactivity decay, that is, a higher density of surface defect states leads to faster photocurrent decay, can be easily verified by the i-t measurements (Figure 1a and b) which exhibit the faster

photocurrent attenuation of D-TiO_2.

In order to provide evidences for the second critical issue, that is, the PEC process will lead to continuous increase of electron transport resistance in TiO_2, a series of combined i-t and potential-step chronoamperometry (PSCA) (Figure s5) and EIS measurements (Figure s6 and s7) are carried out. As seen in Figure s7c, these measurements prove that prolonging the PEC process will continuously deteriorate electron transport property. As we proposed, these decays are attributed to the continuous occurrence of the ETPU process.

As far as electron mobility is not changed, for a given system of nanostructured semiconductor/electrolyte in dark condition R_{tr} can only be varied with Fermi level (electron density).[20,26] However, the current research suggest electron mobility can be continuously changed. Two possible factors may be the origin of this change. One is that the trapping-detrapping events dominate the transport when Fermi level is below the transport edge.[38-40] The other is that the detrapping energy barrier may be increased due to the electrostatic attraction between trapped electrons and protons as well as other cations. For nanostructured TiO_2, the interface transfer of holes is at nanosecond regime while electron transport in TiO_2 is markedly slow,[41] which certainly will cause electron trapping and consequent ETPU. Therefore, along with the proceeding of PEC process the continuous occurrence of ETPU leads to continually increase of transport resistance shown in Figure s7c, which we believe is the essential cause for the general and continuous photoactivity decay typically shown in Figure 1.

It should be stated that other cations in electrolyte may also have the tendency to take part in a similar “electron trapping” induce uptake process. While, considering the smallest diameter and quite strong polarizing power of proton, it is more likely ETPU to be usually the dominant process in various photoelectrochemical systems. This viewpoint can be supported by recent reports although they did not investigate the mechanism of the proton uptake.[42,43] The existence of surface defect states is inevitable for nanostructured inorganic semiconductors, which is why R-TiO_2 still shows slow photocurrent decay despite of its single crystal nature. Moreover, proton charge compensation uptake is also common for many other metal oxides.[28] The above factors make us further propose that the negative influence of ETPU on photoactivity should be general in various non-TiO_2 PEC systems, which needs to be confirmed with more experimental evidences.

4. Conclusion

This work displayed a continuous and reversible photocurrent decay which is general for nanostructured TiO_2 photoelectrodes. During the proceeding of photo/electrochemical process electrons are trapped in surface defect states, leading to electrostatic adsorbing of protons from electrolyte. The electrostatic interactions undermine electron transport property probably by increasing energy barrier for

electron detrapping, which consequently leads to the continuous photocurrent decay.

Acknowledgment

This work was supported by NSFC (Grant No. 21171144), NSF of Shandong province (Grant No. ZR2013EMQ004), the Basic and Frontier Technical Research Project of Henan Province (Grant No. 152300410228) and the University Innovation Team Project in Henan Province (Grant No. 15IRTSTHN004), China.

Reference

(1) Grätzel, M. Dye-sensitized solar cells. *J. Photochem. Photobiol. C* **2003**, *4*, 145-153.

(2) Hoffmann, M. R.; Martin, S. T.; Choi, W. Y.; Bahnemann, D. W. Environmental applications of semiconductor photocatalysis. *Chem. Rev.* **1995**, *95*, 69-96.

(3) Linsebigler, A. L.; Lu, G. Q.; Yates, J. T. Photocatalysis on TiO_2 surfaces: principles, mechanisms, and selected results. *Chem. Rev.* **1995**, 95, 735-758.

(4) Daghrir, R.; Drogui, P.; Robert, D. Modified TiO_2 for environmental photocatalytic applications: a review. *Ind. Eng. Chem. Res.* **2013**, *52*, 3581−3599.

(5) Ochiaia, T.; Fujishima, A.; Photoelectrochemical properties of TiO_2 photocatalyst and its applications for environmental purification. *J. Photochem. Photobiol. C* **2012**, *13*, 247-262.

(6) Fujishima, A.; Honda, K. Electrochemical photolysis of water at a semiconductor electrode. *Nature* **1972**, *238*, 37-38.

(7) Osterloh, F. E. Inorganic nanostructures for photoelectrochemical and photocatalytic water splitting. *Chem. Soc. Rev.*, **2013**, *42*, 2294-2320.

(8) Swierka, J. R.; Mallouk, T. E. Design and development of photoanodes for water-splitting dye-sensitized photoelectrochemical cells. *Chem. Soc. Rev.*, **2013**, *42*, 2357-2387.

(9) Jang, H. D.; Kim, S. K.; Chang, H.; Roh, K.; Choi, J.; Huang, J. A glucose biosensor based on TiO_2-Graphene composite. *Biosensors & bioelectronics*, **2012**, *38*, 184-188.

(10) Dai, H.; Zhang, S.; Hong, Z.; Li, X.; Xu, G.; Lin, Y.; Chen, G. Enhanced Photoelectrochemical Activity of a Hierarchical-Ordered TiO_2 Mesocrystal and Its Sensing Application on a Carbon Nanohorn Support Scaffold. *Anal. Chem.*, **2014**, *86*, 6418–6424.

(11) Berger, T.; Monllor-Satoca, D.; Jankulovska, M.; Lana-Villarreal, T.; Gómez, R. The electrochemistry of nanostructured titanium dioxide electrodes. *ChemPhysChem* **2012**, *13*, 2824-2875.

(12) Monllor-Satoca, D.; Gómez, R. A photoelectrochemical and spectroscopic study of phenol and catechol oxidation on titanium dioxide nanoporous electrodes. *Electrochim. Acta* **2010**, *55*, 4661-4668.

(13) Yu, J.; Wang, B. Effect of calcination temperature on morphology and photoelectrochemical properties of anodized titanium dioxide nanotube arrays. *Appl. Catal. B* **2010**, *94*, 295-302.

(14) Hagfeldt, A.; Lindström, H.; Södergren, S.; Lindquist, S.-E. Photoelectrochemical studies of colloidal TiO_2 films: The effect of oxygen studied by

photocurrent transients. *J. Electroanal. Chem.* **1995**, *381*, 39-46.
(15) Bard, A. J.; Bocarsly, A. B.; Fan, F. F.; Walton, E. G.; Wrighton, M. S. The Concept of Fermi Level Pinning at Semiconductor/Liquid Junctions. Consequences for Energy Conversion Efficiency and Selection of Useful Solution Redox Couples in Solar Devices *J. Am. Chem. Soc.* **1980**, *102*, 3671-3677.
(16) Sivula, K. Metal Oxide Photoelectrodes for Solar Fuel Production, Surface Traps, and Catalysis *J. Phys. Chem. Lett.* **2013**, *4*, 1624-1633.
(17) Thorne, J. E.; Li, S.; Du, C.; Qin, G.; Wang, D. Energetics at the Surface of Photoelectrodes and Its Influence on the Photoelectrochemical Properties *J. Phys. Chem. Lett.* **2015**, *6*, 4083-4088.
(18) Formal, F. L.; Pendlebury, S. R.; Cornuz, M.; Tilley, S. D.; Grätzel, M.; Durrant, J. R. Back Electron−Hole Recombination in Hematite Photoanodes for Water Splitting. *J. Am. Chem. Soc.* **2014**, *136*, 2564−2574.
(19) Klahr, B.; Gimenez, S.; Fabregat-Santiago, F.; Hamann, T.; Bisquert, J. Water Oxidation at Hematite Photoelectrodes: The Role of Surface States. *J. Am. Chem. Soc.* **2012**, *134*, 4294−4302.
(20) Fabregat-Santiago, F.; Mora-Seró, I.; Garcia-Belmonte, G.; Bisquert, J. Cyclic voltammetry studies of nanoporous semiconductors. capacitive and reactive properties of nanocrystalline TiO_2 electrodes in aqueous electrolyte. *J. Phys. Chem. B* **2003**, *107*, 758-768.
(21) Agrell, H. G.; Boschloo, G.; Hagfeldt, A. Conductivity Studies of Nanostructured TiO_2 Films Permeated with Electrolyte. *J. Phys. Chem. B* **2004**, *108*,12388-12396.
(22) Liu, Y.; Hagfeldt, A.; Xiao, X. R.; Lindquist, S-E. Investigation of influence of redox species on the interfacial energetics of a dye-sensitized nanoporous TiO_2 solar cell. *Sol. Energ. Mat. Sol. C.* **1998**, *55*, 267-281.
(23) Liu, B.; Aydil, E. S. Growth of oriented single-crystalline rutile TiO_2 nanorods on transparent conducting substrates for dye-sensitized solar cells. *J. Am. Chem. Soc.* **2009**, *131*, 3985−3990.
(24) He, T.; Weng, Y.; Yu, P.; Liu, C.; Lu, H.; Sun, Y.; Zhang, S.; Yang, X.; Liu, G. Bio-template mediated in situ phosphate transfer to hierarchically porous TiO_2 with localized phosphate distribution and enhanced photoactivities. *J. Phys. Chem. C* **2014**, *118*, 4607-4617.
(25) Yu, J. C.; Zhang, L.; Zheng, Z.; Zhao, J. Synthesis and characterization of phosphated mesoporous titanium dioxide with high photocatalytic activity. *Chem. Mater.* **2003**, *15*, 2280−2286.
(26) Bisquert, J. Chemical capacitance of nanostructured semiconductors: its origin and significance for nanocomposite solar cells. *Phys. Chem. Chem. Phys.* **2003**, *5*, 5360-5364.
(27) Jankulovska, M.; Berger, T.; Wong, S. S.; Gómez, R.; Lana-Villarreal, T. Trap states in TiO_2 films made of nanowires, nanotubes or nanoparticles: an electrochemical study. *ChemPhysChem* **2012**, *13*, 3008-3017.
(28) Lemon, B. I.; Hupp, J. T. Electrochemical quartz crystal microbalance studies of electron addition at nanocrystalline tin oxide/water and zinc oxide/water interfaces: Evidence for band-edge-determining proton uptake. *J. Phys. Chem. B* **1997**, *101*,

2426-2429.
(29) Peters, C. A.; Redmon, B. C. Phenolphthalein and methyl orange. *J. Chem. Educ.* **1940**, 17, 525-528.
(30) Boschloo, G.; Fitzmaurice, D. Electron accumulation in nanostructured TiO_2 (*anatase*) electrodes. *J. Phys. Chem. B* **1999**, *103*, 7860-7868.
(31) O'Regan, B.; Grätzel, M.; Fitzmaurice, D. Optical electrochemistry I: steady-state spectroscopy of conduction-band electrons in a metal oxide semiconductor electrode. *Chem. Phys. Lett.* **1991**, *183*, 89-93.
(32) Fabregat-Santiago, F.; Barea, E. M.; Bisquert, J.; Mor, G. K.; Shankar, K.; Grimes, C. A. High Carrier Density and Capacitance in TiO_2 Nanotube Arrays Induced by Electrochemical Doping. *J. Am. Chem. Soc.* **2008**, *130*, 11312-11316.
(33) Wang, Q.; Zhang, Z.; Zakeeruddin, S. M.; Grä1tzel, M. Enhancement of the performance of dye-sensitized solar cell by formation of shallow transport levels under visible light illumination. *J. Phys. Chem. C* **2008,** *112,* 7084-7092
(34) Idígoras, J.; Berger, T.; Anta, J. A. Modification of mesoporous TiO_2 films by electrochemical doping: impact on photoelectrocatalytic and photovoltaic performance. *J. Phys. Chem. C* **2013**, *117*, 1561-1570.
(35) Lindström, H.; Södergren, S.; Solbrand, A.; Rensmo, H.; Hjelm, J.; Hagfeldt, A.; Lindquist, S.-E. Li^+ Ion Insertion in TiO_2 (Anatase). 2. Voltammetry on Nanoporous Films. *J. Phys. Chem. B* **1997**, *101*, 7717-7722.
(36) Kőrösi, L.; Papp, S.; Bertóti, I.; Dékány, I. Surface and bulk composition, structure, and photocatalytic activity of phosphate-modified TiO_2. *Chem. Mater.* **2007**, *19*, 4811-4819.
(37) Hadjiivanov, K.; Klissurski, D.; Davydov, A. A. Study of phosphate-modified TiO_2 (*anatase*). *J. Catal.* **1989**, *116*, 498-505.
(38) Villanueva-Cab, J.; Jang, S.-R.; Halverson, A. F.; Zhu, K.; Frank, A. J. Trap-free transport in ordered and disordered TiO_2 nanostructures. *Nano Lett.* **2014**, *14*, 2305-2309.
(39) de Jongh, P. E.; Vanmaekelbergh, D. Trap-limited electronic transport in assemblies of nanometer-size TiO_2 particles. *Phys. Rev. Lett.* **1996**, *77*, 3427-3430.
(40) Nelson, J.; Haque, S. A.; Klug, D. R.; Durrant, J. R. Trap-limited recombination in dye-sensitized nanocrystalline metal oxide electrodes. *Phys. Rev. B* **2001**, *63*, 205321.
(41) Kopidakis, N.; Benkstein, K. D.; van de Lagemaat, J.; Frank, A. J. Temperature dependence of the electron diffusion coefficient in electrolyte-filled TiO_2 nanoparticle films: Evidence against multiple trapping in exponential conduction-band tails. *Phys. Rev. B* **2006**, *73*, 045326.
(42) Swierk, J. R.; McCool, N. S.; Saunders, T. P.; Barber, G. D.; Mallouk, T. E. Effects of electron trapping and protonation on the efficiency of water-splitting dye-sensitized solar cells. *J. Am. Chem. Soc.*, **2014**, *136*, 10974-10982.
(43) Halverson, A. F.; Zhu, K.; Erslev, P. T.; Kim, J. Y.; Neale, N. R.; Frank, A. J. Perturbation of the electron transport mechanism by proton intercalation in nanoporous TiO_2 films. *Nano Lett.* **2012**, *12*, 2112-2116.